

ACTIVE MAGNETIC CONTROL SYSTEM FOR  
GRAVITY GRADIENT STABILIZED SPACECRAFT

by Francois Martel, Parimal K. Pal, ITHACO, Inc.  
and Mark Psiaki, Cornell University

ABSTRACT

Active magnetic control is studied as a means to improve the capabilities and performance of gravity gradient stabilized spacecraft.

Active magnetic control eliminates the need for a passive damper and can reduce significantly the costs and complexity of other functional parts of the spacecraft. The system under study includes three magnetic torquers, one three-axis magnetometer, and a control processor. It does not require any moving parts, and provides for rapid libration damping, tighter stabilization and active control of the yaw angle.

Control algorithms are defined. Results of the analysis of the control laws and computer simulations, including high-order models of the geomagnetic field and atmospheric disturbance torques, are presented. The algorithms perform well within a wide range of orbital inclinations and attitude angles and allow maneuverability and stabilization around the yaw axis.

A Kalman Filter is used to provide estimates of the attitude angles, the angular rates, and a global disturbance torque, based on measurements from the magnetometer. Results of simulations, including the attitude estimator in the control loop, are presented. The possibility of a fully autonomous acquisition, deployment, and stabilization sequence using the magnetic control system is discussed.

## INTRODUCTION

### Background on Gravity Gradient Stabilization

The use of gravity gradient provides a simple way to stabilize a spacecraft in a Nadir pointing mode. An extendable boom is generally used to provide adequate moments of inertia and a damping mechanism is required to reduce the libration motions.

A gravity gradient system is bi-stable, and the acquisition procedure must be carefully performed to avoid a stabilization upside-down. Since that does happen, the extendable boom is often designed to be retractable, to allow for the possibility of reversing the spacecraft.

A momentum wheel is sometimes added to the system for three-axis stabilization and better pointing performance, with the additional benefit of providing a mechanism for stabilization in two possible opposite "yaw" angular positions around the Nadir direction. Proper ratios of the moments of inertia provide another way for stabilization in two possible fixed yaw positions.

Generally a gravity gradient system is slow to stabilize, and has limited pointing capabilities; the boom structure is affected by thermal gradients which alters the overall attitude of the spacecraft; the maneuvers for capture of the gravity gradient require extensive ground support; there is very limited or no control of the yaw attitude angle around the Nadir direction.

Arbitrary control of the yaw angle would be desirable for thermal management of the spacecraft (control of the orientation of spacecraft surfaces with respect to the sun direction; uniformization of exposure of the boom structure to solar radiation to avoid unwanted thermal gradients resulting in bending); or for improvement of the power or communication systems trade-offs through better capability for orientation of fixed solar panels or antennas; or for orientation of sensitive payload sensors away from the sun line, etc.

### Application of Active Magnetic Control

The addition of active magnetic control to a gravity gradient stabilized system appears as a means to increase the system capabilities and performance while improving the overall cost trade-offs. An active magnetic control system can provide very effective, rapid and tighter damping, and replace the passive dampers. It does not require any moving parts; it can provide for automatic initial acquisition and stabilization of the spacecraft in a spin control mode after launch; it can be used for attitude and angular rate measurements and automatic gravity gradient capture; the magnetic torqueing capabilities can be used for reversal for the spacecraft when necessary, and provide the capability for arbitrary control of the spacecraft yaw angle.

In addition such an active control system allows a relaxation of the requirements on the gravity gradient boom; the boom does not need to be retractable and its thermal characteristics are less critical.

The understanding of the advantages of such system led to detailed studies of adequate attitude determination and control algorithms for its implementation. These algorithms were specified to provide for attitude determination, automatic libration damping, and arbitrary yaw control with instrumentation limited to a three-axis magnetometer, three magnetic torquers, and a control microprocessor.

This document discusses the results of the study of the application of an active magnetic control to gravity gradient stabilized satellites conceived for a multiple satellite system. In the first part, the system and the control method are described and analyzed. The results of realistic simulations are then presented and discussed. Finally, the general description of a possible method for autonomous deployment sequence of the spacecraft is presented.

## SYSTEM DESCRIPTION

The proposed system consists of three main parts: a magnetometer to measure the local magnetic field at the spacecraft, a set of three magnetic torquers, and a control electronics assembly based on a microcomputer.

A general diagram of the system is shown in Figure 1. The three components of the magnetic field  $B_x$ ,  $B_y$ ,  $B_z$  are read and processed by the microcomputer, which then communicates control commands to the magnetic torquer driver. The magnetic torquer driver provides the selected current levels to the magnetic torquer coils, generating the desired magnetic dipole moments,  $M_x$ ,  $M_y$ ,  $M_z$  in the three axis. These dipoles interact with the earth magnetic field to generate a controlled torque to the spacecraft.

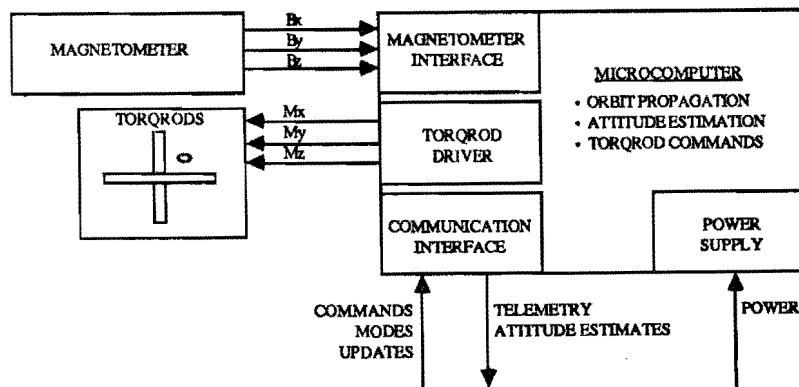


Figure 1: Magnetic Control System - Hardware Configuration

The system communicates to the spacecraft telemetry to receive commands or data and send status and data. The control system is conceived to be as autonomous as possible and commands may be limited to mode selection, while the data consists of a periodic reset of the spacecraft orbital parameters for the propagation procedures.

## ATTITUDE DETERMINATION AND CONTROL ALGORITHMS

Several approaches were explored to meet the goal of achieving three-axis attitude stabilization and control of the spacecraft yaw angle using the minimal amount of instrumentation of the system (a three-axis magnetometer and three magnetic torquers).

### Control Method

Simple control algorithms were initially considered. The classical damping control laws simply based on the measurement of the magnetic field rates of change in the spacecraft reference frame are generally successful in damping relatively rapid motions. Such laws, with proper gains, are applicable in the initial attitude acquisition period, to despin or detumble the spacecraft.

The same simple laws are not effective for final three-axis stabilization of the spacecraft, because of the effect of the orbital rates, and the non-uniformity of the geomagnetic field.

If a perfect knowledge of the earth magnetic field is assumed, the spacecraft libration motion can be damped very effectively with a control law such as

$$\underline{M} = -K_1(\underline{B} - \underline{B}_0) - K_2(\dot{\underline{B}} - \dot{\underline{B}}_0)$$

where  $\underline{M}$  is the dipole moment,  $\underline{B}$  is the measured magnetic field vector,  $\underline{B}_0$  is the magnetic field model vector in orbital frame, and  $K_1$  and  $K_2$  are restoring and damping factors.

With such law the simulated attitude angles can be brought to null in three axes when no disturbances are considered. However, in these ideal conditions, the yaw axis although stabilized, is still not maneuverable. Moreover, the system does not handle large angular excursions well.

One important requirement for the system is the capability for a good level of angular control about the yaw axis, in order to be able to rotate the satellite. Performing yaw control to various angles requires information on the spacecraft yaw angle in order to apply the proper torques to the platform.

The actual attitude angles are not readily available from the field measurements. They can be extracted though, by proper filtering of the measurement data on extended time periods, especially if the spacecraft dynamic properties are known well. In particular, a Kalman estimator, using a good geomagnetic field model, can perform the task of estimating the three Euler angles and their rates from the magnetic field measurement only.

Such an attitude estimator based on a Kalman filter was developed to provide estimates of the Euler angles, the angular rates and a slow varying disturbance torque, to the system controller.

To perform attitude estimates from the magnetic field measurements, a model of the local geomagnetic field is used for comparison with the measured values. Such a model can be accurately computed by the system microcomputer, if the spacecraft position is known. The spacecraft position is calculated by propagation from initial orbital parameters. Because of aerodynamic drag the orbit decays in time. The on-board propagation algorithms need to be updated periodically to compensate for the unpredicted orbital disturbances. Updates can be provided from a ground station or derived from a GPS receiver on-board the spacecraft.

The Kalman filter is described in Reference 1. It was tested in simulations including atmospheric, solar radiation and residual magnetic disturbance torques, as well as realistic parameter and measurement errors.

To define and test control algorithms suitable for the control goals, it can then be assumed that estimates of the Euler angles and their rates and of a global disturbance torque are available to the control system. Effective control rules can be developed on this basis as described in the following section. Figure 2 shows a conceptual diagram of such system.

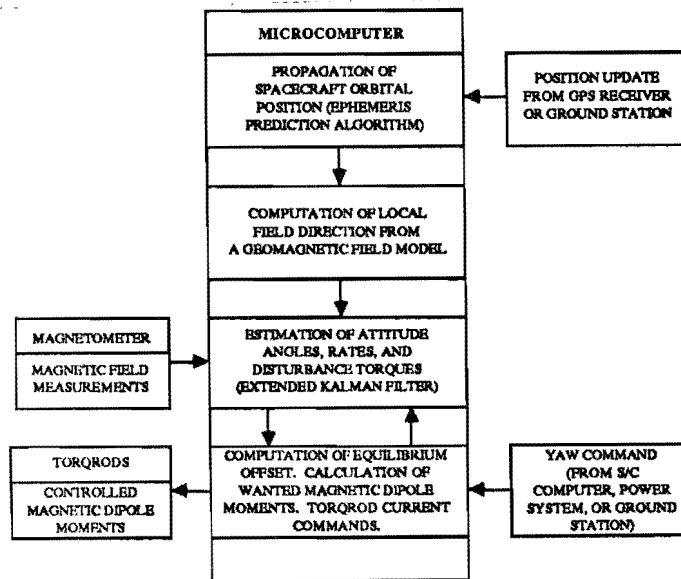


Figure 2: Conceptual Diagram of the Magnetic Attitude Determination and Control System

### Description of the Proposed Control Laws

Using the assumption that reasonable values for the three Euler angles, roll ( $\phi$ ), pitch ( $\theta$ ), and yaw ( $\psi$ ) and their rates are available, a straightforward control method can be devised. The convention used here assumes the roll angular motion around the X body axis (nominally along the velocity vector), the pitch angular motion around the Y axis (nominally along the negative orbit normal) and the yaw angular motion around the Z axis (nominally in the Nadir direction). The selected Euler rotation sequence is 3-1-2 (i.e., Z-X-Y) with the respective angles  $\Psi, \phi, \theta$ .

An "error correction" vector is defined as:

$$\mathbf{m} = K_p \cdot (\mathbf{a} - \text{bias}) + K_d \cdot \dot{\mathbf{a}}$$

where  $K_p$  and  $K_d$  are the diagonal matrices of the proportional and derivative gains associated with the restoring and damping torques. The vectors  $\mathbf{a}$  and  $\dot{\mathbf{a}}$  have for components the Euler angles and their rates respectively. i.e.,

$$\mathbf{a} = \begin{bmatrix} \phi \\ \theta \\ \psi \end{bmatrix}, \dot{\mathbf{a}} = \begin{bmatrix} \dot{\phi} \\ \dot{\theta} \\ \dot{\psi} \end{bmatrix}$$

and the vector **bias** includes typically a pitch equilibrium offset based on the estimated offset disturbance torque ( $T_D$ ) and a yaw command:

$$\text{Bias} = \begin{pmatrix} 0 \\ \text{Pitch Offset } (T_D) \\ \text{Yaw Command} \end{pmatrix}$$

The desired correction torques expressed in  $\underline{m}$  can only be actuated inasmuch as the local magnetic field direction is favorable. The local field vector  $\underline{B}_B$  is measured by the on-board magnetometer. To take the magnetic field direction into account the commanded dipole moment vector is defined as:

$$\underline{M} = \frac{\underline{m} \times \underline{B}_B}{|\underline{B}_B|}$$

The local field vector where  $\underline{B}_B$  is measured by the on-board magnetometer.

The actual torques applied to the spacecraft are generated by the interaction of the dipole moment vector  $\underline{M}$  with the earth's field vector  $\underline{B}_B$  and are given by the components of the vector

$$\underline{T} = \underline{M} \times \underline{B}_B$$

As shown in a next subsection, these control laws apply torques with proper polarity about all the three-axes. The relation between the desired torques and the actual torques depend on the field orientation. Since the field orientation vary along the orbit, favorable configurations can be found for period of times, allowing the system to stabilize, in a wide range of orbital inclinations.

#### Linear Analysis of the Magnetic Control Laws

An analysis of the control law was done with linearized equations of motion, assuming small angular excursions.

The linearized equations of motion are given by:

$$\begin{aligned} I_x \ddot{\phi} + 4\omega_0^2 (I_y - I_z) \phi - (I_x - I_y + I_z) \omega_0 \dot{\psi} &= T_{CX} + T_{DX} \\ I_y \ddot{\theta} + 3\omega_0^2 (I_x - I_z) \theta &= T_{CY} + T_{DY} \\ I_z \ddot{\psi} + \omega_0^2 (I_y - I_x) \psi + (I_x - I_y + I_z) \omega_0 \dot{\phi} &= T_{CZ} + T_{DZ} \end{aligned} \quad (1)$$

where

$I_x, I_y, I_z$  are the Moment of Inertia about X, Y, Z axes respectively,  
 $\omega_0$  is the orbital rate,  
 $T_{CX}, T_{CY}, T_{CZ}$  (as derived below) are the magnetic control torques, and  
 $T_{DX}, T_{DY}, T_{DZ}$  are the disturbance torques about the X, Y and Z axes respectively.

The desired control torques for the three-axes are defined from the Euler angles and their rates using the Proportional/Derivative (PD) law:

$$\begin{aligned} m_x &= K_{PX} \phi + K_{DX} \dot{\phi} \\ m_y &= K_{PY} \theta + K_{DY} \dot{\theta} \\ m_z &= K_{PZ} \psi + K_{DZ} \dot{\psi} \end{aligned} \quad (2)$$

where  $(K_{PX}, K_{PY}, K_{PZ})$  and  $(K_{DX}, K_{DY}, K_{DZ})$  are the proportional and derivative gains respectively, for the three axes.

To apply the magnetic torques about the corresponding axes, magnetic dipole moments ( $M_x, M_y, M_z$ ) are distributed along the other body axes according to the following rule

$$\underline{M} = \begin{bmatrix} M_x \\ M_y \\ M_z \end{bmatrix} = \underline{m} \times \underline{h} = \begin{bmatrix} m_y b_z - m_z b_y \\ m_z b_x - m_x b_z \\ m_x b_y - m_y b_x \end{bmatrix} \quad (3)$$

where  $\underline{M}$  is the desired dipole vector,  $\underline{m} = \begin{bmatrix} m_x \\ m_y \\ m_z \end{bmatrix}$  and  $\underline{h}$  is the normalized earth's magnetic field vector in body

$$\text{frame defined as } \underline{h}(\varphi, \theta, \psi) = \frac{\underline{B}(\varphi, \theta, \psi)}{|\underline{B}|}$$

Thus, the actual control torques about the body axes ( $T_{cx}, T_{cy}, T_{cz}$ ) are given by:

$$\underline{T}_c = \begin{bmatrix} T_{cx} \\ T_{cy} \\ T_{cz} \end{bmatrix} = \underline{M} \times \underline{B}(\varphi, \theta, \psi) = \frac{1}{|\underline{B}|} \begin{bmatrix} -(B_y^2 + B_z^2) & B_x B_y & B_x B_z \\ B_x B_y & -(B_x^2 + B_z^2) & B_y B_z \\ B_x B_z & B_y B_z & -(B_x^2 + B_y^2) \end{bmatrix} \begin{bmatrix} m_x \\ m_y \\ m_z \end{bmatrix} \quad (4)$$

$$= \frac{1}{|\underline{B}|} \cdot L(\underline{B}) \cdot \underline{m} \quad (5)$$

Equation (4) shows that with the dipole moments defined by (3) the control torques have the right polarity associated with the diagonal term of the  $L(\underline{B})$  matrix. The off diagonal terms show some undesirable coupling effects due to torquing about the other axes.

With a small angle assumption the body-fixed field vector  $\underline{B}$  vector can be written as:

$$\underline{B} = A(\varphi, \theta, \psi) \underline{B}^0 = \begin{bmatrix} 1 & \psi & -\theta \\ -\psi & 1 & \varphi \\ \theta & -\varphi & 1 \end{bmatrix} \underline{B}^0, \text{ with } \underline{B}^0 = \begin{bmatrix} B_x^0 \\ B_y^0 \\ B_z^0 \end{bmatrix} \quad (6)$$

where  $A$  is the direction cosine matrix and  $\underline{B}^0$  is the earth's magnetic field vector in the orbital frame.

The lengths of  $|\underline{B}|$  and  $|\underline{B}^0|$  are equal and the elements in the  $L(\underline{B})$  matrix of equation (4) can be approximated as follows (because of the small angle assumption):

$$\begin{aligned} B_y^2 + B_z^2 &\cong (B_y^0)^2 + (B_z^0)^2 & B_x B_y &\cong B_x^0 B_y^0 \\ B_x^2 + B_z^2 &\cong (B_x^0)^2 + (B_z^0)^2 & B_x B_z &\cong B_x^0 B_z^0 \\ B_x^2 + B_y^2 &\cong (B_x^0)^2 + (B_y^0)^2 & B_y B_z &\cong B_y^0 B_z^0 \end{aligned}$$

Thus, the matrix  $L(\underline{B})$  can be approximated by  $L(\underline{B}^0)$  and the control torque  $\underline{T}_C$  in (4) using (2), can be approximated by the vector:

$$\underline{T}_C \equiv L(\underline{B}^0) \cdot \underline{m} / |\underline{B}| \quad (7)$$

Using (7), the equations of (1) can be written as:

$$\begin{aligned} I_x \ddot{\phi} + 4\omega_0^2 (I_y - I_z) \phi + \frac{((B_y^0)^2 + (B_z^0)^2)}{|\underline{B}^0|} \cdot [K_{PX}\phi + K_{DX}\dot{\phi}] - \frac{B_x^0 \cdot B_y^0}{|\underline{B}^0|} (K_{PY}\theta + K_{DY}\dot{\theta}) \\ - \frac{B_x^0 \cdot B_z^0}{|\underline{B}^0|} (K_{PZ}\psi + K_{DZ}\dot{\psi}) - (I_x - I_y + I_z) \omega_0 \dot{\psi} &= T_{DX} \\ I_y \ddot{\theta} + 3\omega_0^2 (I_x - I_z) \theta + \frac{((B_x^0)^2 + (B_z^0)^2)}{|\underline{B}^0|} (K_{PY}\theta + K_{DY}\dot{\theta}) - \frac{B_x^0 \cdot B_y^0}{|\underline{B}^0|} (K_{PX}\phi + K_{DX}\dot{\phi}) \\ - \frac{B_y^0 \cdot B_z^0}{|\underline{B}^0|} (K_{PZ}\psi + K_{DZ}\dot{\psi}) &= T_{DY} \\ I_z \ddot{\psi} + \omega_0^2 (I_y - I_x) \psi + \frac{((B_x^0)^2 + (B_z^0)^2)}{|\underline{B}^0|} (K_{PZ}\psi + K_{DZ}\dot{\psi}) - \frac{B_x^0 \cdot B_z^0}{|\underline{B}^0|} (K_{PX}\phi + K_{DX}\dot{\phi}) \\ - \frac{B_y^0 \cdot B_z^0}{|\underline{B}^0|} (K_{PY}\theta + K_{DY}\dot{\theta}) + (I_x - I_y + I_z) \omega_0 \dot{\phi} &= T_{DZ} \end{aligned} \quad (8)$$

The vector  $\underline{B}^0$  is quasi periodic, at the orbital period  $T_p$ . The elements of  $\underline{B}^0$  may be replaced by their orbital averages to perform an approximate stability analysis, using standard linear time invariant techniques. (A Floquet analysis of the exact closed loop stability of this periodic system has been performed; it shows that parametric resonance instability can occur for certain gain values, for which the average analysis indicates stability with a low damping ratio. However, average coefficient analysis is adequate when the close loop time constants are not too fast.)

The quantities  $\frac{(B_i^0)^2 + (B_j^0)^2}{|\underline{B}^0|}$  and  $\frac{B_i^0 \cdot B_j^0}{|\underline{B}^0|}$  can then be replaced by the orbital average values

$$\alpha_{ij} = \frac{1}{T_p} \int_0^{T_p} \frac{(B_i^0)^2 + (B_j^0)^2}{|\underline{B}^0|} dt, \quad i \neq j = x, y, z$$

and,

$$\beta_{ij} = \frac{1}{T_p} \int_0^{T_p} \frac{B_i^0 \cdot B_j^0}{|\underline{B}^0|} dt, \quad i \neq j = x, y, z$$



Taking the Laplace transformation of the equations in (8) gives:

$$\Delta(s) \cdot \underline{a}(s) = \underline{T}_D(s) \quad (9)$$

where

$$\Delta(s) = \begin{bmatrix} a_{11}s^2 + a_{12}s + a_{13} & -(b_{11} + b_{12}s) & -(c_{11} + c_{12}s) \\ -(d_{11} + d_{12}s) & a_{21}s^2 + a_{22}s + a_{23} & -(e_{11} + e_{12}s) \\ -(f_{11} + f_{12}s) & -(g_{11} + g_{12}s) & a_{31}s^2 + a_{32}s + a_{33} \end{bmatrix}$$

$$\underline{a}(s) = \begin{bmatrix} \varphi(s) \\ \theta(s) \\ \psi(s) \end{bmatrix}, \text{ and } \underline{T}_D(s) = \begin{bmatrix} T_{DX}(s) \\ T_{DY}(s) \\ T_{DZ}(s) \end{bmatrix}$$

The a, b, c, d, e, f, g constants in  $\Delta(s)$  are functions of the spacecraft mass properties,  $\alpha_{ij}$ ,  $\beta_{ij}$ ,  $\omega^0$  and the controller gains  $K_p$  and  $K_d$ .

Alternatively, (9) can be rewritten as:

$$\underline{a}(s) = \Delta^{-1}(s) \times \underline{T}_D(s) \quad (10)$$

It is to be noted from (8) that even though the linearized pitch equation of motion is not coupled with the roll/yaw motions in the absence of control torque, the magnetic control torques generate cross coupling and the characteristic polynomial is of the sixth order.

For this analysis the atmospheric drag force is assumed to be a constant force  $F$  acting on the spacecraft center of pressure along the negative velocity vector with an amplitude  $F_x$ . With the small angle assumptions, the force vector along the body axes is given by:

$$\underline{F}^B = \begin{bmatrix} F_x^B \\ F_y^B \\ F_z^B \end{bmatrix} = \begin{bmatrix} -F_x \\ \psi F_x \\ -\theta F_x \end{bmatrix} \quad (11)$$

If the offset vector between the center of pressure and the center of gravity is defined as  $\underline{\gamma} = \begin{bmatrix} \gamma_x \\ \gamma_y \\ \gamma_z \end{bmatrix}$ ,

the disturbance torques about the three axes are defined by the vector

$$\underline{T}_D = \underline{\gamma} \times \underline{F}^B = \begin{bmatrix} -(\gamma_y \theta + \gamma_z \psi) F_x \\ -(\gamma_z - \theta \gamma_x) F_x \\ (\gamma_y + \psi \gamma_x) F_x \end{bmatrix} = \begin{bmatrix} T_{DX} \\ T_{DY} \\ T_{DZ} \end{bmatrix} \quad (12)$$

or taking the Laplace Transformation

$$\mathbf{T}_D(s) = \begin{bmatrix} T_{DX}(s) \\ T_{DY}(s) \\ T_{DZ}(s) \end{bmatrix} = \begin{bmatrix} -\{\gamma_y \theta(s) + \gamma_z \cdot \psi(s)\} F_x \\ -\left\{ \frac{\gamma_z}{s} - \theta(s) \cdot \gamma_x \right\} F_x \\ \left\{ \frac{\gamma_y}{s} + \psi(s) \cdot \gamma_x \right\} F_x \end{bmatrix} \quad (13)$$

From (11) we derive:

$$\varphi(s) = \frac{1}{|\Delta(s)|} [\Delta_{11}(s) \cdot T_{DX}(s) + \Delta_{12}(s) \cdot T_{DY}(s) + \Delta_{13}(s) \cdot T_{DZ}(s)]$$

Where the coefficients  $\Delta_{ij}(s)$  are the cofactors of  $\Delta(s)$ .

The steady-state value of  $\varphi$ , say  $\varphi_{SS}$  is given by

$$\varphi_{SS} = \lim_{s \rightarrow 0} s\varphi(s) = \frac{(E_0\gamma_x - B_0\gamma_y)F_x}{A_0} \cdot \theta_{SS} + \frac{(F_0\gamma_x - B_0\gamma_z)F_x}{A_0} \cdot \psi_{SS} + \frac{(F_0\gamma_y - E_0\gamma_z)F_x}{A_0} \quad (16)$$

where  $A_0, B_0, E_0, F_0$  are functions of the spacecraft mass properties, the field vector and the control gains.  $\theta_{SS}$  and  $\psi_{SS}$  are the steady state values of  $\theta$  and  $\psi$ .

Similarly the expressions corresponding to  $\theta$  and  $\psi$  are

$$\begin{aligned} \theta_{SS} [A_0 + (G_0\gamma_y - C_0\gamma_x)F_x] + F_x(G_0\gamma_x - I_0\gamma_x)\psi_{SS} &= (I_0\gamma_y - C_0\gamma_z)F_x \\ \theta_{SS} [(H_0\gamma_y - J_0\gamma_x)F_x] + [A_0 + (H_0\gamma_z - D_0\gamma_x)F_x]\psi_{SS} &= (D_0\gamma_y - J_0\gamma_z)F_x \end{aligned} \quad (15)$$

Once  $\theta_{SS}$  and  $\psi_{SS}$  are found from (15),  $\varphi_{SS}$  can be calculated from (14).

For the present analysis the parameter values are assumed as follows:

$$\begin{aligned} I_x &= I_y = 250 \text{ Kg-m}^2 \\ I_z &= 10 \text{ Kg-m}^2 \\ \omega_0 &= 0.00107 \text{ rad} \end{aligned}$$

The  $\alpha$  and  $\beta$  values are considered for three different inclination of  $80^\circ$ ,  $57^\circ$  and  $28.5^\circ$ , at an altitude of 364.5 nm. These values are calculated from an eighth-order model geomagnetic field and are listed in Table 1:

| $\alpha, \beta$ | $i = 80^\circ$            | $i = 57^\circ$            | $i = 28.5^\circ$          |
|-----------------|---------------------------|---------------------------|---------------------------|
| $\alpha_{xy}$   | $1.37659 \times 10^{-5}$  | $1.67488 \times 10^{-5}$  | $2.43338 \times 10^{-5}$  |
| $\alpha_{xz}$   | $3.50276 \times 10^{-5}$  | $2.75481 \times 10^{-5}$  | $1.08617 \times 10^{-5}$  |
| $\alpha_{yz}$   | $2.78432 \times 10^{-5}$  | $2.84181 \times 10^{-5}$  | $2.83197 \times 10^{-5}$  |
| $\beta_{xy}$    | $-3.47527 \times 10^{-7}$ | $-3.70462 \times 10^{-7}$ | $-3.84555 \times 10^{-7}$ |
| $\beta_{xz}$    | $-8.55599 \times 10^{-7}$ | $-7.26248 \times 10^{-7}$ | $-5.05008 \times 10^{-7}$ |
| $\beta_{yz}$    | $1.41729 \times 10^{-6}$  | $9.64049 \times 10^{-7}$  | $7.12059 \times 10^{-8}$  |

Table 1:  $\alpha$  and  $\beta$  Values as a Function of Inclination  $i$

Using the characteristic equation  $|\Delta(s)| = 0$  from (9) with no control ( $K_P = 0, K_D = 0$ ), the roots of the system are:

$$\begin{aligned} &(\pm 2.105 \times 10^{-3} j) \\ &(\pm 1.802 \times 10^{-3} j) \\ &(0,0) \end{aligned}$$

associated with the roll, pitch, and yaw axes respectively. These roots indicate that in the absence of control the roll and pitch angles are undamped and oscillating and the yaw angle is unstable.

With the proposed control laws for an orbital inclination of  $57^\circ$  and using the following gain values:

$$\begin{aligned} K_{PX} &= K_{PY} = 25 \\ K_{PZ} &= 8 \\ K_{DX} &= K_{DY} = K_{DZ} = 25000 \end{aligned}$$

the corresponding roots are:

$$\begin{aligned} &-1.747 \times 10^{-3} \pm 2.292 \times 10^{-3} j \\ &-1.721 \times 10^{-3} \pm 2.022 \times 10^{-3} j \\ &\text{and } (-3.224 \times 10^{-4}, -3.971 \times 10^{-2}) \end{aligned}$$

The negative real parts of all the roots show that the proposed magnetic control law makes the yaw angle stable with a time constant of 3100 sec. The roll and pitch angle oscillations are damped with time constants of 572 secs. and 581 secs. respectively. The longer time constant for yaw can be seen in all the simulation plots.

With the same gains, similar results can be seen for other inclinations, viz.,

$$\begin{aligned} \text{for } i = 80^\circ, \text{ the roots are} & \quad (-1.389 \times 10^{-3} \pm 2.30 \times 10^{-3} j) \\ & \quad (-1.73 \times 10^{-3} \pm 1.93 \times 10^{-3} j) \\ & \quad (-3.230 \times 10^{-4}, -3.411 \times 10^{-2}) \end{aligned}$$

$$\begin{aligned} \text{and for } i = 28.5^\circ, \text{ the roots are} & \quad (-1.416 \times 10^{-3} \pm 2.278 \times 10^{-3} j) \\ & \quad (-5.422 \times 10^{-3} \pm 2.016 \times 10^{-3} j) \\ & \quad (-3.217 \times 10^{-4}, -6.050 \times 10^{-2}) \end{aligned}$$

With a constant disturbance force of  $7.11 \times 10^{-6}$  Newton and a CP-CG offset of 2.8 m along the z axis and 6 cm along the other axes, i.e.,  $F_x = 7.11 \times 10^{-6}$  Newton and  $\gamma_x = \gamma_y = 0.06$  m,  $\gamma_z = -2.8$  m, the steady-state bias can be calculated from (15) and (17) and are found to be

$$\begin{aligned} \varphi_{ss} &= 0.0024 \text{ rad} \\ \theta_{ss} &= 0.0132 \text{ rad} \\ \psi_{ss} &= -4.93 \times 10^{-5} \text{ rad} \end{aligned}$$

The pitch bias error  $\theta_{ss}$  is, of course, the most significant and can be noticed in the simulation plots.

In conclusion, the control laws defined in this section are shown as effective and stable from an analysis based on the linearized equations of angular motion, and average field parameters integrated along the orbit path using an eighth order geomagnetic field model. The system is applicable with identical gains at the three orbital inclinations proposed for the MSS satellites ( $28.5^\circ$ ,  $57^\circ$  and  $80^\circ$ ). Additional time domain simulations in the next section confirm this analysis and provide a more detailed description of the expected performance of the system.

## TIME DOMAIN SIMULATIONS

Time domain simulations were performed to assess the system capabilities in different configurations. A block diagram of the attitude simulation program is presented in Figure 3.

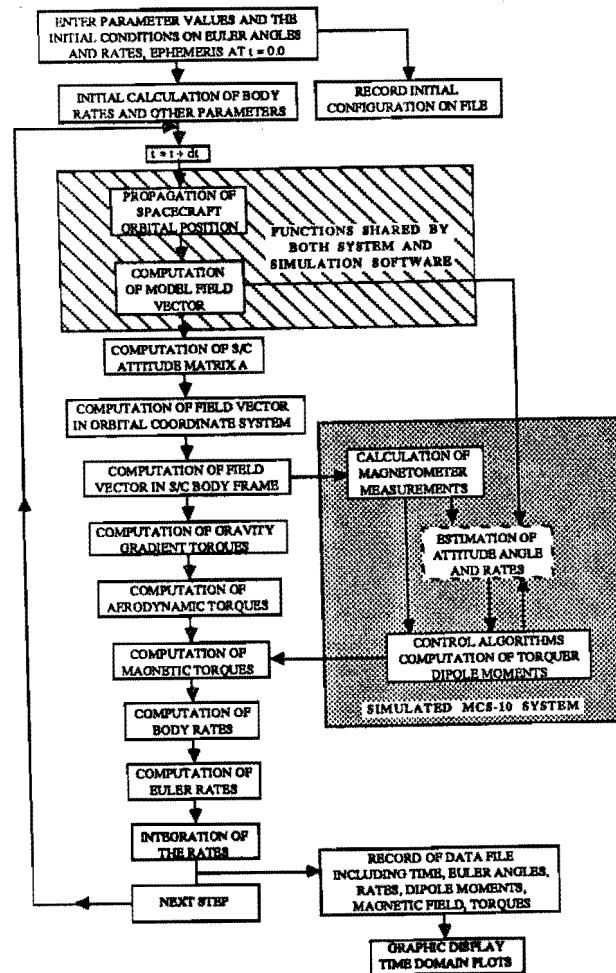


Figure 3: Block Diagram of the Numerical Simulation Program

The program allows for selection of the moment of inertia, initial attitude and angular rates, restoring and damping gains, orbital parameters, order of the magnetic field model, maximum magnetic moment, atmospheric disturbance torque coefficients, and components of the offset vector between the center of gravity and center of pressure of the spacecraft. Selected attitude offsets and measurement noises can be entered in the simulations.

The program propagates the spacecraft orbital position, computes the local geomagnetic field in earth-fixed coordinates from an eighth-order magnetic field model, and calculates the field components in the orbital coordinate system and the spacecraft body fixed-coordinate frame. The gravity gradient and aerodynamic torques on the spacecraft are calculated and added to the magnetic torques generated by the magnetic control system. (Other disturbance torques such as solar radiation torque or residual magnetic dipole torques were not included in this study since their effect is secondary and system design dependent.) The control system simulation modules have for inputs the local magnetic field model in orbital frame and the field vector as "measured" in the spacecraft body frame, and for output the dipole moments of the controlled magnetic torquers.

The shaded blocks in Figure 3 correspond to the functions which are to be performed on board the spacecraft. For the initial testing it was assumed that accurate estimates of the attitude angles and their rates were provided to the control algorithms. Subsequent testing included the extended Kalman filter estimator, as source of the attitude estimates within the control loop.

Body rates and Euler rates are computed and integrated using a variable step Runge Kutta integration procedure. Fields and torques are computed for every substep of the integration. The control commands however, are computed at regular intervals of typically 20 seconds.

The simulated atmospheric drag torques use a simple disturbance model. The simulated torque is either constant or made to vary at orbital rate between a minimum and maximum value. The selected values correspond to atmospheric densities at 364.5 nmiles in 1992, close to the peak of the solar cycle, derived from the Jacchia atmospheric model. They are very conservative, if not a "worst case". The geomagnetic field is computed through an eighth-order spherical harmonic model using coefficients listed in the IGRF tables.

The selected spacecraft parameters are derived from estimates of the spacecraft mechanical design and mass properties using indications from the MSS program phase A report presentations.

The spacecraft is assumed to be of cylindrical shape with a total weight of 136 Kg. The spacecraft's moment of inertia used for the simulations are (with no product of inertia):

|         |          |   |                       |
|---------|----------|---|-----------------------|
| (Roll)  | $I_{xx}$ | = | 250 Kg-m <sup>2</sup> |
| (Pitch) | $I_{yy}$ | = | 250 Kg-m <sup>2</sup> |
| (Yaw)   | $I_{zz}$ | = | 10 Kg-m <sup>2</sup>  |

The cylinder has a height of 4 feet with a radius of 14". The spacecraft is assumed to be in circular orbit at the altitude of 675 Km and in three possible orbital inclinations of 28.5°, 57°, and 80°. The maximum boom and boom mass area which are subject to aerodynamic pressure are assumed to correspond to 10% of the spacecraft body area similarly exposed. The torque generating aerodynamic force is assumed to be typically applied to a point 2.8 m (or 6 m) along the z axis from the center of gravity and generated by an effective area of 0.93 ft<sup>2</sup> (0.0867 m<sup>2</sup>). From a conservative analysis of atmospheric density at the altitude of 675 Km, the mean, maximum and minimum atmospheric forces along the orbit are taken to be  $7.1 \times 10^{-6}$ ,  $10.65 \times 10^{-6}$ , and  $4.7 \times 10^{-6}$  Newtons respectively. The force is assumed to be periodic with periodicity equal to the orbital period of  $\omega_0$ . The periodic force F is modelled as:

$$F = F_0 \gamma \cos(\omega_0 t) \quad , \quad \gamma = 1.5 \quad , \quad F_0 = 7.11 \times 10^{-6} \text{ N}$$

### Simulation Results

To test the performance of the proposed magnetic control law, a number of time-domain simulation runs were made under a wide variety of conditions. The configurations tested in the simulations include:

- Different Orbital Inclinations
- Different Initial Conditions for Attitude Angles and Rates
- Different Initial Hour Angle
- Yaw Angle Maneuver and Control
- Stabilization with Large Aerodynamic Torques
  - with the CP-CG vector along the yaw axis
  - with the CP-CG vector tilted away from the yaw axis

The nominal gains for the control laws were selected by iterative simulations. The chosen gains are applicable in a wide range of inclinations. The nominal gains may be adjusted sometimes, to handle the disturbance torque more efficiently in given inclinations.

The simulations confirmed the stability analysis. The magnetic control system is able to damp most of the libration motion within an orbit. Figure 4 and 5 show typical attitude angles trajectories for initial excursions in yaw, roll and pitch of 1 radian and 0.1 radian in the absence of disturbance torques.

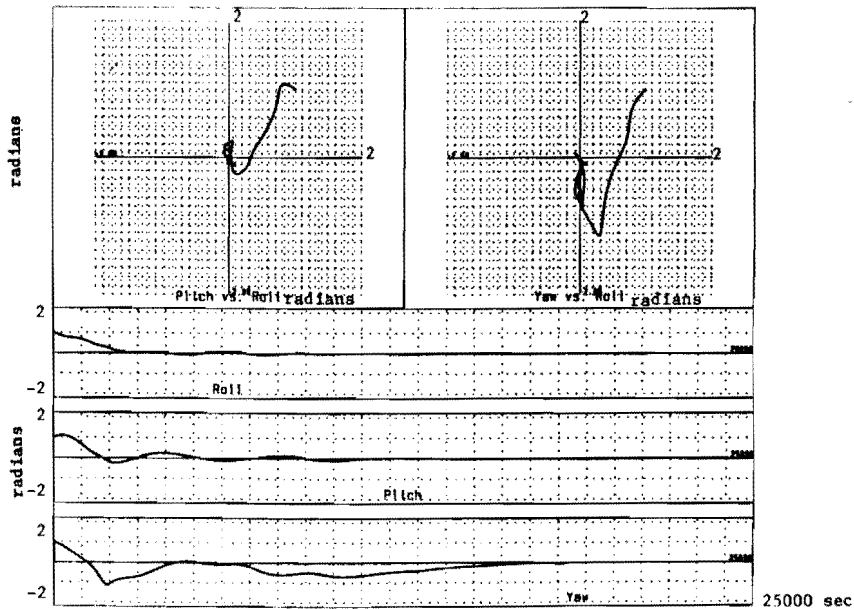


Figure 4: Attitude Histories for  $i = 57^{\circ}$ , No Disturbance, Initial Condition = 1 rad in Each Axis

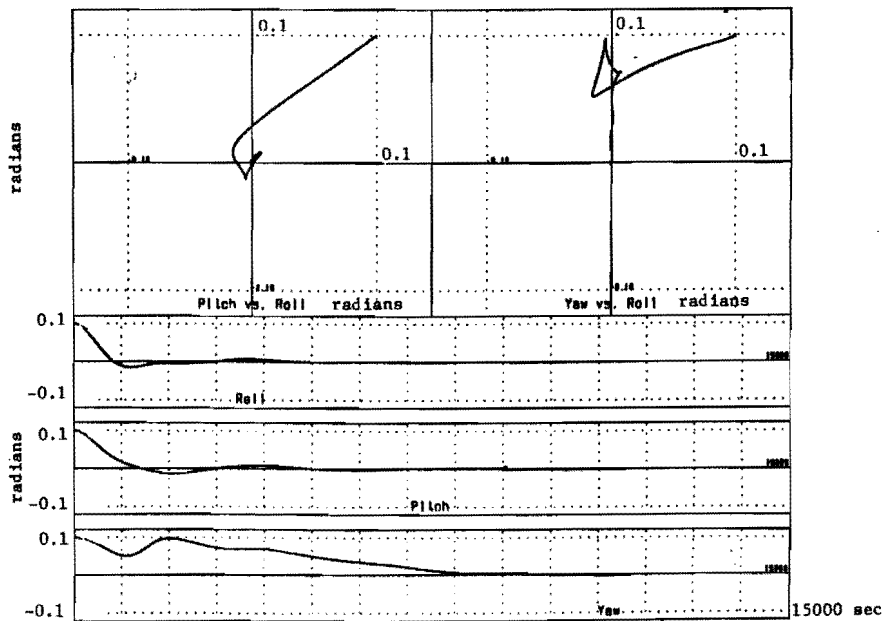


Figure 5: Attitude Histories for  $i = 57^{\circ}$ , No Disturbance, Initial Condition = 0.1 rad in Each Axis

The damping is less effective but still adequate for low orbital inclinations as witnessed in Figure 6 because the magnetic field configuration is less favorable at these inclinations.

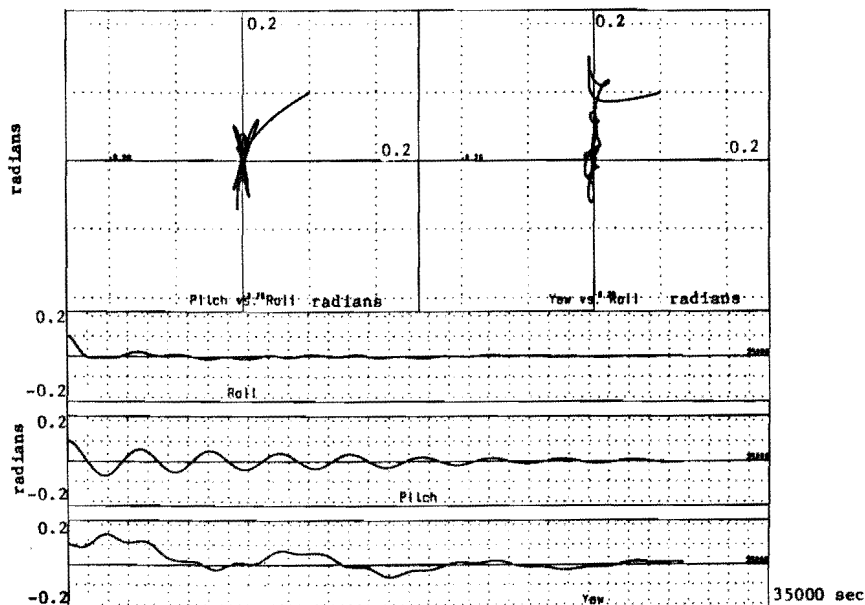


Figure 6: Attitude Histories for  $i = 28.5^{\circ}$ , No Disturbance Torque, Initial Condition = 0.1 rad in Each Axis.

In the presence of strong atmospheric disturbance torques, there are times when the field configuration does not allow effective nulling of the pitch angle. To minimize limit cycle oscillations, an equilibrium offset bias can be calculated from the disturbance torque estimates. The controller then tries to achieve stabilization around the bias angle instead of null. Figure 7 shows the attitude angles histories for a configuration including large variable atmospheric disturbances. A constant average bias is applied to the pitch command. The small oscillation around the pitch equilibrium could be further reduced by varying the bias command according to the estimated disturbance torque.

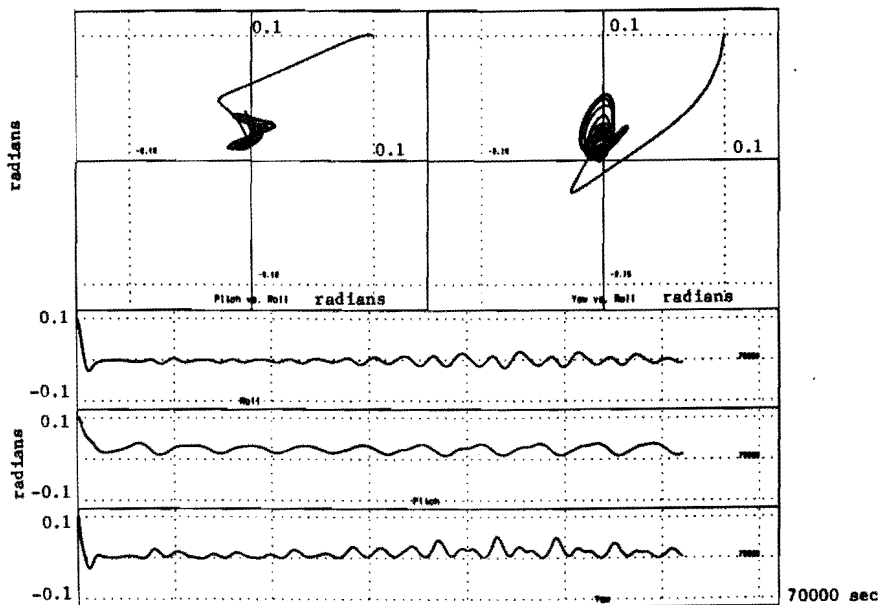


Figure 7: Attitude Histories,  $i = 57^{\circ}$ , With Disturbance, CP-CG Offset = -2.8 m Along z axis, 6 cm Along x, y, Pitch Bias = 0.02 rad.



An example of 180° yaw maneuver is shown in Figure 8 and Figure 9 in the absence and presence of the atmospheric disturbances and with different restoring gains.

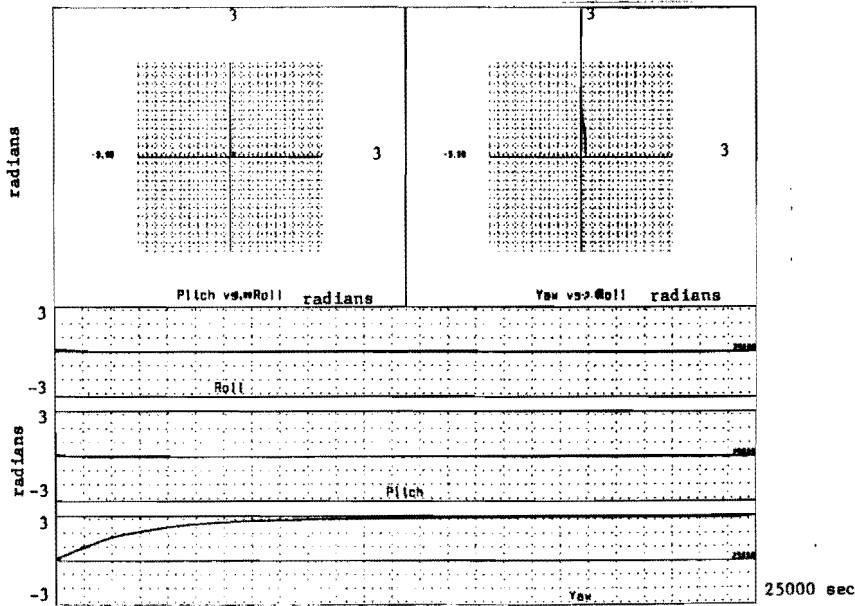


Figure 8: Yaw Maneuver of the Spacecraft to 180° with  $i = 57^\circ$ , No Disturbance

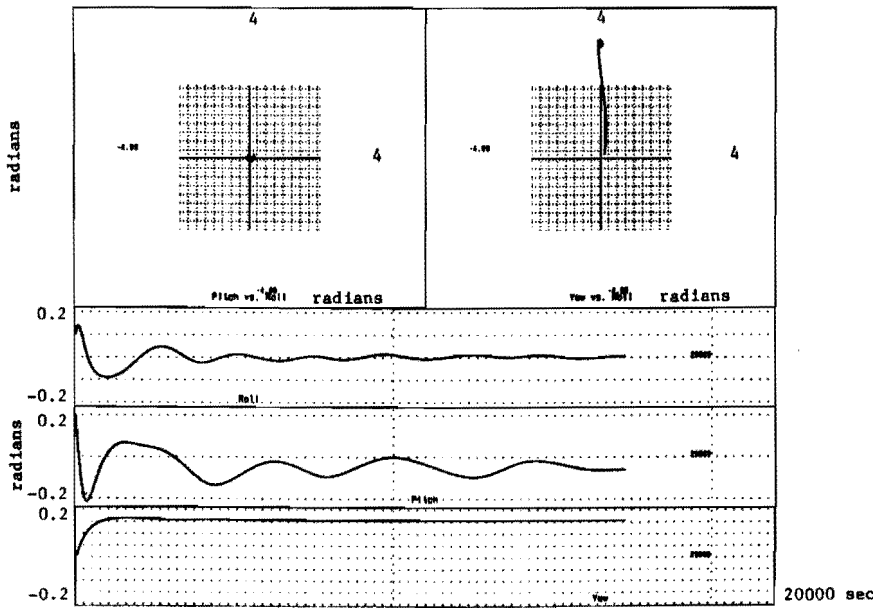


Figure 9: Yaw Maneuver History with Disturbance Torque,  $i = 57^\circ$ , CP-CG Offset = -2.8 m Along z Axis, 6 cm Along x, y, Pitch Bias = 0.024 rad.

The previous examples were assuming the availability of precise attitude estimates for the controller.

## Conclusion

Active magnetic attitude determination and control can provide significant enhancement in the capabilities and performances of gravity gradient stabilized spacecraft. Requiring no moving parts and no expendables, the method eliminates the need for passive damper and may relax the thermal and mechanical requirements on the gravity gradient boom. It provides the possibility for automatic execution of the attitude acquisition and boom deployment maneuvers and therefore can relieve the ground station of resource consuming tasks. The added abilities for attitude determination, and control of the yaw angle open the system trade-offs for improved mission capabilities or reduced system costs. These advantages are achieved at the expense of additional on-board processing, with the need for periodic orbital updates.

A set of algorithms for magnetic attitude control was defined, analyzed and tested in simulations. The results indicate that such algorithms can perform well the required tasks, in conjunction with previously designed attitude estimation algorithms.

## ACKNOWLEDGEMENTS

This work was supported in part by ITHACO, Inc., and by the Defense Advanced Research Project Agency under contract F29601-87-C-0051.

## BIBLIOGRAPHY

### References and Bibliography

1. "Three-Axis Attitude Determination via Kalman Filter of Magnetometer Data," by Francois Martel, Parimal K. Pal, and Mark L. Psiaki, Paper No. 17, Flight Mechanics/Estimation Theory Symposium, NASA/Goddard Space Flight Center, Greenbelt Maryland, May 10-11, 1988.
2. "An Elementary Magnetic Attitude Control System," by A. Craig Stickler and K. T. Alfriend, AIAA Mechanics and Control of Flight Conference, Anaheim, California, August 5-9, 1974.
3. "Spacecraft Attitude Determination and Control," by J. Wertz, P. Reidel Publishing Company.